



# Combining geodetic data and summer MODIS albedo anomalies for annual glacier mass balance estimation

Mattia Callegari<sup>1</sup>, Carlo Marin<sup>1</sup>, Claudia Notarnicola<sup>1</sup>, Thomas Schellenberger<sup>2</sup>

<sup>1</sup>Institute for Earth Observation, Eurac Research, Viale Druso, 1, 39100 Bolzano, Italy

5 <sup>2</sup>Department of Geosciences, University of Oslo, Oslo, 0316, Norway

*Correspondence to:* Mattia Callegari (mattia.callegari@eurac.edu)

**Abstract.** Annual glacier mass balance time series are essential for understanding the impacts of climate change on glacierized regions. Satellite-based observations enable consistent and regionally comprehensive monitoring of glacier mass balance. While geodetic methods provide reliable estimates over decadal timescales, deriving accurate annual glacier mass balance estimates remains challenging. In this study, we propose a new approach that combines 20 years geodetic mass balance data with glacier-wide average summer albedo anomalies from MODIS to produce reliable annual glacier mass balance estimates for land-terminating glaciers. We generated time series from 2000 to 2024 for 2748 glaciers across three regions: the European Alps, Scandinavia, and Svalbard. Validation against 1108 available in-situ mass balance measurements yielded root mean square errors (RMSE) of 0.45, 0.79, and 0.42 m w.e. and coefficients of determination ( $R^2$ ) of 0.60, 0.44, and 0.35 for the European Alps, Scandinavia, and Svalbard, respectively. These results demonstrate the method's effectiveness and its potential for application in other glacierized regions.

## 1 Introduction

Glaciers are sensitive indicators of climate change, and their annual mass balance provides a critical metric for understanding their response to changing climatic conditions. Annual glacier mass balance represents the net gain or loss of glacier snow and ice over a hydrological year and is essential for assessing the contributions of glaciers to sea-level rise, freshwater resources, and regional hydrology (Hugonnet et al., 2021; Huss & Hock, 2018; Marzeion et al., 2012; Zemp et al., 2019; The GlaMBIE Team, 2025).

Approaches to estimating glacier mass balance can be broadly categorized into in-situ measurements, physical models, and satellite-data-based methods. In-situ measurements, i.e. the glaciological method, provide accurate, site-specific data, but are labor-intensive and limited in spatial and temporal coverage (Cogley et al., 2011). Physical models simulate glacier mass balance using meteorological and topographic inputs (Maussion et al., 2019), offering broad applicability but relying heavily on accurate input data, which may not always be available. Satellite-based methods, by contrast, enable regional to global coverage and consistent temporal monitoring, though they often face challenges related to data temporal and spatial resolution and the need for calibration (Rabatel et al., 2017).



30 Among satellite-based methods, the geodetic approach, which measures elevation changes from satellite or airborne data to  
infer mass balance, has become a cornerstone in glacier monitoring. Hugonnet et al. (2021) demonstrated the value of multi-  
decadal geodetic datasets in quantifying global glacier mass changes with unprecedented precision. Their dataset is based on  
digital elevation models (DEMs) generated primarily from imagery acquired by the Advanced Spaceborne Thermal Emission  
and Reflection Radiometer (ASTER), onboard the NASA's Terra satellite and operational since 2000. ASTER provides 30-  
35 meter resolution stereo imagery, enabling the creation of DEMs over mountainous and glacierized regions. However, due to  
limitations in ASTER's radiometric and geometric accuracy, the resulting DEMs are not sufficiently precise to support  
reliable annual glacier mass balance estimates. Consequently, the Hugonnet dataset is restricted to multi-year or decadal  
timescales, where longer temporal windows help suppress measurement noise. While this improves robustness, it leaves a  
critical gap in the temporal resolution needed to capture short-term glacier responses to climatic variability.

40 An effective approach to estimate annual glacier mass balance from multi-year geodetic measurements involves using the  
snowline altitude (SLA) as a proxy for the equilibrium line altitude (ELA), a key indicator of glacier mass balance (Davaze  
et al., 2020; Rabatel et al., 2005, 2012, 2016). The ELA method relates the end-of-summer snowline position, derived from  
optical satellite imagery to the annual mass balance of glaciers and has been successfully applied in various mountain  
regions. However, its accuracy can be limited by persistent cloud cover, data gaps, and cases where the ELA exceeds the  
45 glacier's maximum elevation, leading to incomplete or unreliable estimates. More recently, Dussailant et al. (2025)  
proposed a complementary approach that integrates satellite-derived geodetic data with in-situ glaciological observations  
through geostatistical temporal downscaling, producing globally consistent annual mass balance time series from 1976 to  
2024. This highlights the potential of combining satellite and ground-based information to enhance the temporal resolution  
of glacier mass balance estimates, but its reliance on in-situ data may reduce performance in regions where field  
50 measurements are sparse or absent.

Numerous studies have demonstrated a strong correlation between glacier-wide surface albedo and mass balance. Albedo  
directly influences the glacier's energy balance by regulating the absorption of solar radiation, which in turn affects melting  
rates. De Ruyter De Wildt et al. (2002) used albedo data from the Advanced Very-High-Resolution Radiometer (AVHRR) to  
estimate the absorbed radiation over the ablation season, averaged across the glacier surface. Their analysis explained 76-  
55 88% of the variance in mass balance for six outlet glaciers of Vatnajökull, Iceland, using linear relationships. Greuell &  
Oerlemans (2005) applied this approach to estimate surface mass balance along the K-transect of the Greenland Ice Sheet  
and later tested it on 18 Svalbard glaciers using Moderate Resolution Imaging Spectroradiometer (MODIS) albedo data  
(Greuell et al., 2007). Dumont et al. (2012) also showed that MODIS albedo captures interannual variability in mass balance  
for Alpine glaciers. Brun et al. (2015) and Sirguey et al. (2016) found high correlation between minimum annual albedo and  
60 mass balance for Himalayan and New Zealand glaciers, with coefficients of determination ( $R^2$ ) of 0.75 and 0.98,  
respectively. Davaze et al. (2018) analyzed MODIS imagery from 2000–2015 and identified significant correlations between  
summer minimum albedo and annual surface mass balance for 30 glaciers in the French Alps. Di Mauro & Fugazza (2022)  
confirmed the robustness of various MODIS-derived albedo metrics against annual mass balance for 31 selected Alpine



glaciers. More recently, Williamson et al. (2025) showed that declining albedo can accelerate glacier mass loss in North  
65 America, with statistically significant correlations between albedo change and mass balance. Despite these promising results,  
most albedo-based approaches have been limited to individual glaciers or small regions, and their scalability to broader  
regional or global applications remains unexplored.

In this study, we propose a novel approach, which we refer to as the albedo-anomaly method, that combines glacier-wide  
summer albedo anomalies derived from MODIS data with geodetic glacier mass balance estimates to produce annual glacier  
70 mass balance estimates at regional scales. The method leverages 20 years geodetic mass balance data (Hugonnet et al., 2021)  
to calibrate the relationship between annual albedo anomalies and mass balance anomalies, enabling the conversion of  
relative anomalies into absolute annual mass balance values.

The proposed method is validated using in-situ glacier mass balance data from the World Glacier Monitoring Service  
(WGMS) across three key regions: the European Alps, Scandinavia, and Svalbard. These regions offer a diverse range of  
75 glacier characteristics and climatic conditions, providing a rigorous testbed for the method.

The paper also presents an open-access time series of annual glacier mass balance for these regions, filling critical gaps in  
regional glacier monitoring. In addition, the codebase for the methodology is published as open access, implemented using  
Google Earth Engine (GEE) to facilitate straightforward application to other mountain ranges worldwide. This contribution  
aims to promote the broader adoption of satellite-based glacier mass balance monitoring and enhance our ability to track and  
80 understand glacier responses on regional to global scale to climate change.

## 2 Study regions

Our study focuses on the estimation of annual glacier mass balance across three regions: the European Alps, Scandinavia,  
and Svalbard (Figure 1). These regions encompass a diverse range of glacial environments, making them well suited for  
assessing large-scale glacier mass balance variability using satellite remote sensing.

85 The European Alps primarily feature temperate valley glaciers, which are characterized by year-round ice movement and  
significant seasonal melt. Alpine glaciers are highly sensitive to climate variability and have experienced substantial retreat  
in recent decades (Zemp et al., 2019), providing an important benchmark for evaluating satellite-derived annual mass  
balance estimates.

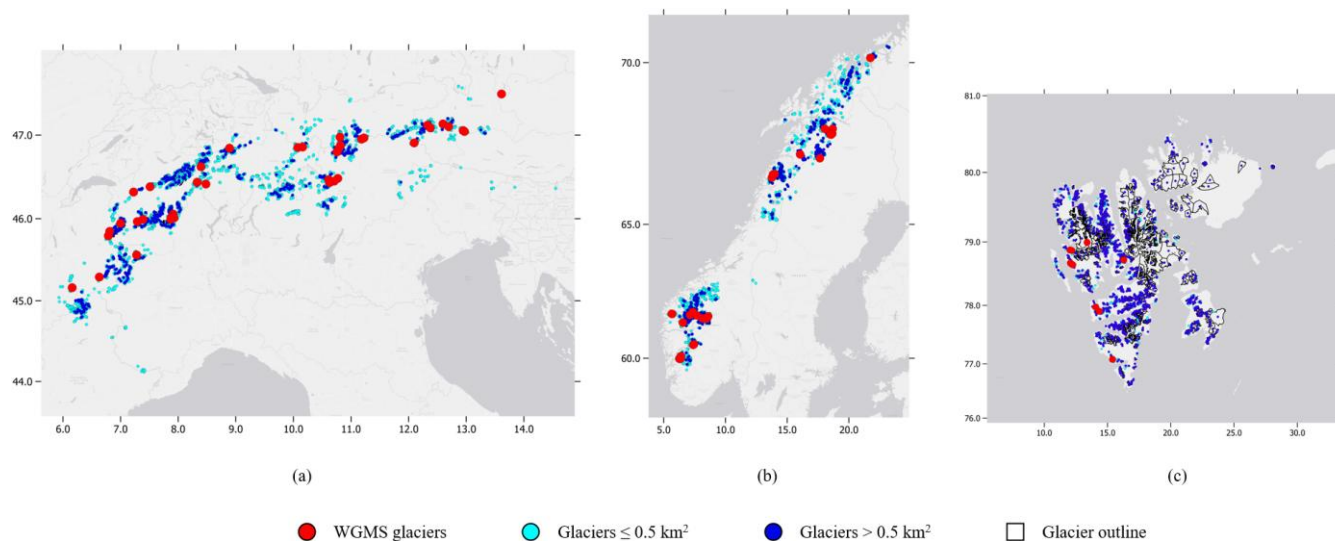
Scandinavia hosts a mixture of maritime and subpolar glaciers, many of which are located along the western coast, where  
90 high precipitation and relatively mild temperatures result in dynamic mass balance conditions (Andreassen et al., 2020). As a  
consequence, Scandinavian glaciers represent a contrasting validation dataset compared to the European Alps, characterized  
by higher accumulation rates and stronger interannual variability.

Further north, in Svalbard, glaciers exhibit a combination of cold-based and polythermal structures, where the presence of  
both frozen and temperate ice layers influences their response to climate change. The glaciers in Svalbard are largely  
95 influenced by Arctic conditions, with prolonged periods of winter accumulation and short, intense melt seasons (Schmidt et



al., 2023). Their distinct thermal structure and surface energy balance make Svalbard glaciers particularly relevant for assessing the transferability of albedo-based approaches to cold and high-latitude environments.

All three regions benefit from a dense network of long-term in situ glacier mass balance observations coordinated by the WGMS, which provides a robust basis for validating the annual mass balance estimates derived in this study.



100

**Figure 1: Overview map of the three study regions: European Alps (a), Scandinavia (b), and Svalbard (c). Red circles represent glaciers with WGMS in-situ measurements of annual glacier mass balance, cyan (blue) circles glacier smaller (bigger) than 0.5 km<sup>2</sup>. Basemap: ESRI Gray | Powered by Esri.**

### 3 Data and methods

105 To estimate annual glacier mass balance, we combined satellite-derived glacier-wide summer albedo with long-term geodetic mass balance data. Under the assumption that annual glacier mass balance anomalies are linearly correlated with glacier-wide summer albedo anomalies, we defined this relationship as:

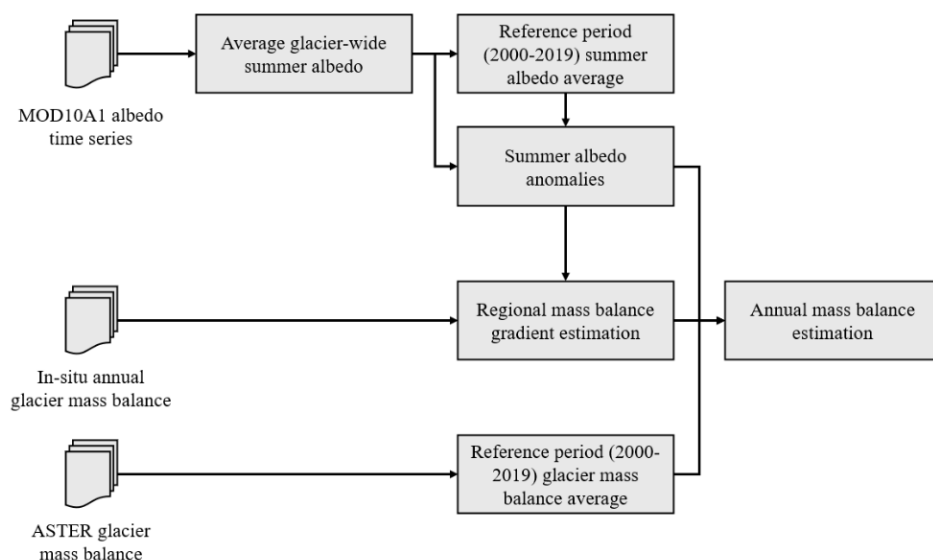
$$B_i - \bar{B} = (\alpha_i - \bar{\alpha}) \frac{db}{d\alpha}, \quad (1)$$

where  $B_i$  is the annual glacier mass balance to be estimated, and  $\alpha_i$  is the glacier-wide summer albedo (1 July–30 September) derived from the MODIS daily snow albedo product MOD10A1 (Hall & Riggs, 2021). The overline ( $\bar{B}$  and  $\bar{\alpha}$ ) indicates the average value of each variable over the reference period 2000-2019. Specifically,  $\bar{B}$  is extracted from digital elevation models (DEMs) (Hugonnet et al., 2021). The parameter  $\frac{db}{d\alpha}$  represents the mass balance anomaly gradient, quantifying the sensitivity of glacier mass balance to variations in albedo. This gradient was determined by applying a linear regression between annual glacier-wide albedo anomalies and annual glacier mass balance anomalies derived from in-situ surface mass balance observations. Although, in principle, a locally fitted gradient for each glacier would yield greater precision, this approach is often not feasible due to the limited availability of in-situ measurements. Conversely, while a

115



global fit may be affected by outliers, a carefully constrained regional derivation, based on glaciers with similar environmental conditions, provides a robust and operationally practical solution. The overall methodological workflow is illustrated in Figure 2.



120

**Figure 2: Schematic overview of the methodological workflow used to estimate annual glacier mass balance.**

### 3.1 Average glacier-wide summer albedo from Terra MODIS

The MODIS sensor on board of NASA’s Terra satellite acquires imagery in 36 spectral bands ranging from visible to thermal infrared, allowing for comprehensive monitoring of Earth’s surface conditions. The MOD10A1 product provides daily snow cover maps and albedo measurements at a 500-meter spatial resolution, derived from MODIS reflectance data in the visible, near-infrared and short-wave-infrared bands (Hall, D. K. & Riggs, G. A., 2021).

Access to the MOD10A1 product and computation of glacier-wide daily albedos were performed using Google Earth Engine (GEE). Specifically, for each day, we calculated the mean albedo of all pixels within glacier outlines from the Randolph Glacier Inventory, RGI v6 (RGI Consortium, 2017), and determined the fraction of valid pixels, where invalid pixels represented cloud cover or missing data. For each glacier, only days for which more than 70 % of the pixels within the glacier outline were valid were retained for the analysis. To maintain a continuous daily time series, gaps in the data were filled using linear interpolation. If the start or end of the time series contained fewer than 70% valid pixels, we used the average albedo from the nearest preceding (for the start) or subsequent (for the end) day that met the threshold, enabling interpolation to be performed across the entire period. The interpolated values were then used to compute the summer mean albedo for the period from 1 June to 30 September. As an illustrative example, Figure 3 shows the procedure applied to the La Mare Glacier, located in the Ortles–Cevedale Group (European Alps), during the 2003 ablation season. Figure 4 presents the glacier-wide summer albedo time series from 2000 to 2024 for the same glacier.

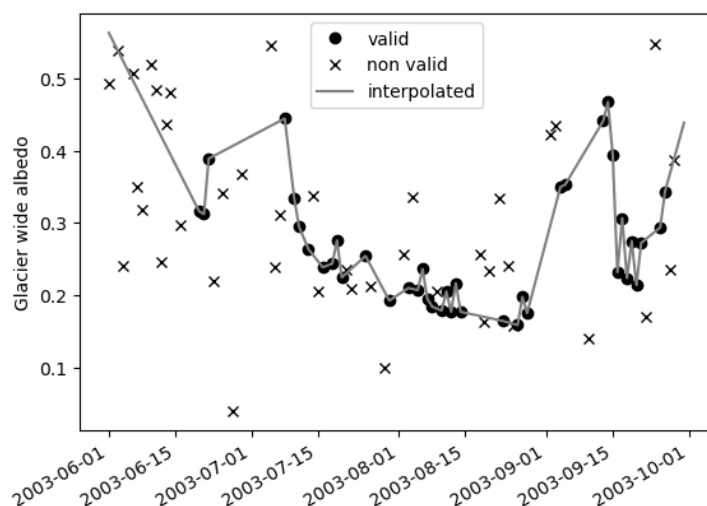
125

130

135



140 We focused on the summer months for three main reasons. First, albedo remains high and relatively stable during the winter accumulation period, so variations in annual albedo are primarily driven by changes during the melting season. Second, albedo measurements are unavailable during the polar night (e.g., in Svalbard), making summer data more accessible and reliable. Third, concentrating on the melting season reduces computational costs while still capturing the most significant variations in albedo.



145 **Figure 3: Daily glacier-wide albedo on the La Mare Glacier (Ortles-Cevedale Group, European Alps) during the 2003 ablation season. Cross markers indicate data points with a valid pixel fraction below the threshold of 70%. Circle markers represent valid glacier-wide albedo values, with the gray line showing the daily interpolation.**

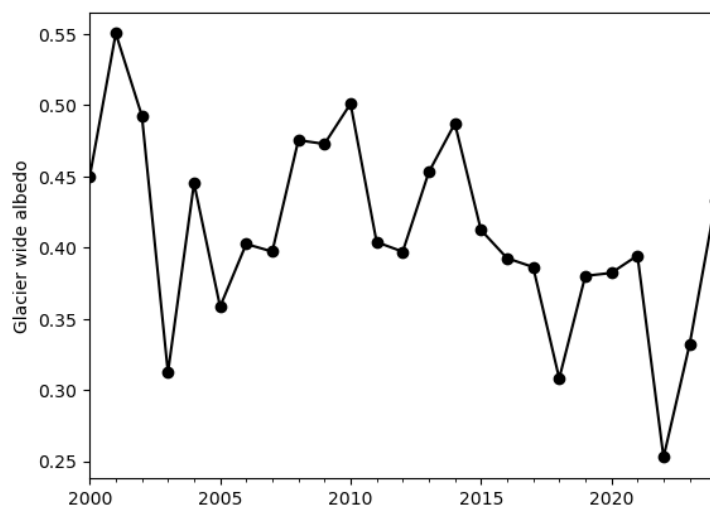


**Figure 4: Mean glacier-wide albedo on La Mare Glacier (Ortles-Cevedale Group, European Alps), averaged annually over the ablation season (June 1st to September 30th) for each year.**



### 150 3.2 Glacier mass balance from repeat DEMs

The 20-year glacier mass balance is assessed using the global glacier elevation change dataset of Hugonnet et al. (2021), which is derived from repeat digital elevation models (DEMs). The primary source of elevation data is the ASTER sensor onboard NASA's Terra satellite, which provides stereoscopic imagery capable of generating DEMs at up to 30 m resolution. In addition, ArcticDEM data are incorporated where available (e.g. Svalbard), improving elevation accuracy in high-latitude regions.

155 The Hugonnet et al. dataset has a spatial resolution of 100 m and spans the period 2000–2019, providing a consistent, long-term record of glacier elevation and mass change. Glacier-specific time series of mass change rates are provided for all glaciers defined in RGI version 6 (RGI Consortium, 2017). While the dataset yields robust estimates of glacier mass balance at decadal timescales, its reliability at annual resolution is limited, as the accuracy is comparable to the magnitude of  
160 observed annual glacier elevation change (Hugonnet et al., 2021).

### 3.3 In-situ annual glacier mass balance measurements

The satellite-derived mass balance estimates were validated by using glaciological measurements (i.e., in-situ observations) from the World Glacier Monitoring Service (WGMS). To ensure compatibility with the MODIS spatial resolution and the reliability of the albedo–mass balance relationship, we excluded glaciers smaller than 0.5 km<sup>2</sup> as well as marine-terminating and surging glaciers. After applying these filters, we retained 39 glaciers in the European Alps, 27 in Scandinavia, and 10 in  
165 Svalbard for the period 2000–2019 (Table 1), ensuring a 20-year overlap with MODIS and DEM acquisitions for validation. Figure 1 shows the spatial distribution of the selected WGMS glaciers across the three study regions.

**Table 1: Summary of in-situ annual glacier mass balance measurements from the World Glacier Monitoring Service (WGMS) used for validation. The table reports the number of glaciers retained after excluding small (<0.5 km<sup>2</sup>), maritime-terminating, and  
170 surging glaciers, along with the total number of annual observations available for the period 2000–2019 in each study region.**

Region name	Number of glaciers used for validation	Number of annual mass balance measurements used for validation
European Alps	39	641
Scandinavia	27	355
Svalbard	10	112

### 3.4 Error metrics for validation with glaciological data

Mean bias error (MBE), mean absolute error (MAE), root mean square error (RMSE) and coefficient of determination ( $R^2$ )  
175 were computed for the comparison between the modelled and in-situ annual mass balance estimates. The following error metrics are defined as:



$$\text{MBE} = \frac{1}{N} \sum_{i=1}^N (y_i - \hat{y}_i), \quad (2)$$

$$\text{MAE} = \frac{1}{N} \sum_{i=1}^N |y_i - \hat{y}_i|, \quad (3)$$

$$\text{RMSE} = \sqrt{\frac{1}{N} \sum_{i=1}^N (y_i - \hat{y}_i)^2}, \quad (4)$$

$$180 \quad R^2 = 1 - \frac{\sum_{i=1}^N (y_i - \hat{y}_i)^2}{\sum_{i=1}^N (y_i - \bar{y})^2}, \quad (5)$$

Where  $N$  is the total number of samples,  $\hat{y}_i$  is the predicted value of the  $i$ -th sample and  $y_i$  is the corresponding true value;

$$\bar{y} = \frac{1}{N} \sum_{i=1}^N y_i.$$

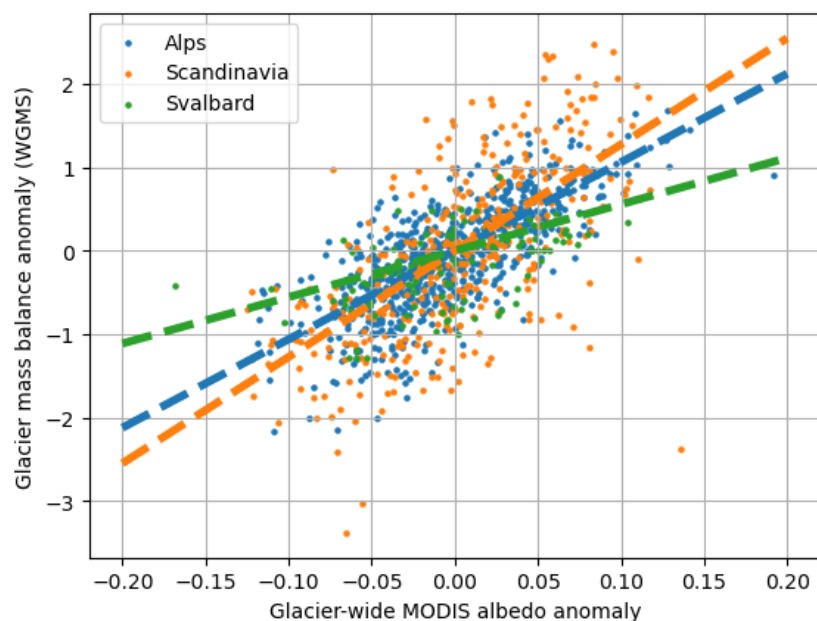
## 4. Results

### 4.1 Mass balance anomaly gradient estimation

185 We tested two approaches to estimate the mass balance anomaly gradient  $\frac{db}{d\alpha}$  (Eq. 1), both based on a linear regression between glacier-wide albedo anomalies and glacier mass balance anomalies derived from in situ measurements.

In the first approach, a single (global) mass balance anomaly gradient was estimated using all available data from the three study regions. This global gradient was then applied to estimate the annual mass balance of all glaciers. Such a setup reflects situations where in situ measurements are available only in neighboring regions, requiring the adoption of a common  
190 gradient due to the lack of local field data. The global gradient obtained from this analysis is 10.93 m w.e..

In the second approach,  $\frac{db}{d\alpha}$  was estimated separately for each study region, resulting in three distinct gradients: one for the European Alps, one for Scandinavia, and one for Svalbard. Figure 5 shows the linear regression relationships obtained for the three regions. The corresponding gradient values are 10.61 m w.e. for the European Alps, 12.73 m w.e. for Scandinavia, and 5.56 m w.e. for Svalbard.



195

**Figure 5: Glacier-wide albedo versus glacier mass balance annual anomalies from WGMS for the glaciers in the European Alps (blue), Scandinavia (orange) and Svalbard (green). Dashed lines represent the linear regression from which the coefficients  $\frac{db}{da}$  have been estimated.**

The global value is close to that of the Alps, likely reflecting the larger number of available samples from this region. Table 2 summarizes the error metrics obtained using both the global and regional gradients. While results for the Alps and Scandinavia show only minor differences, larger discrepancies are observed for Svalbard, likely due to its distinct climatic conditions and glaciological processes compared to the other regions. These results indicate that gradients derived from neighboring glaciers can yield reasonable estimates when local data are unavailable, although the approach performs best when neighboring regions share similar climatic conditions.

To assess the robustness and spatial representativeness of using a single regional gradient, we conducted a leave-one-out cross-validation (LOOCV) experiment. In this test, the regional analysis was repeated iteratively: in each iteration, all glaciers within the same region except one were used to estimate the mass balance anomaly gradient. This gradient was then applied to the excluded glacier to reconstruct its specific glacier mass balance time series, which was subsequently compared with observations to compute error metrics. The gradients obtained through LOOCV range from 10.41 to 10.78 m w.e. in the European Alps, from 11.93 to 13.93 m w.e. in Scandinavia, and from 4.98 to 6.64 m w.e. in Svalbard (Figure 6). These comparatively narrow ranges do not lead to any meaningful variation in the corresponding error metrics computed on the specific glacier mass balance estimation (Table 2), confirming the robustness of the method and supporting the applicability of a single regional gradient to represent an entire glacierized region.

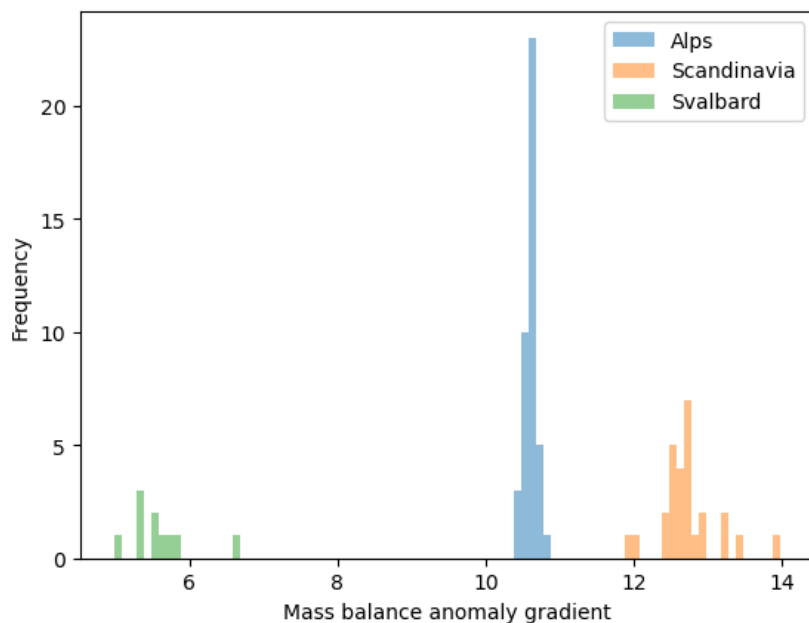
**Table 2: Error metrics associated with the estimation of annual glacier mass balance using the global gradient, the regionally derived gradient, and the leave-one-out cross-validation (LOOCV) gradient for the three study regions. Metrics include mean bias**

215



error (MBE), mean absolute error (MAE), root-mean-square error (RMSE), and the coefficient of determination ( $R^2$ ), all expressed relative to in situ mass balance measurements.

Region	Number of validation samples	Error metric	Global gradient	Regional gradient	Regional LOOCV
European Alps	641	MBE (m w.e.)	-0.04	-0.05	-0.05
		MAE (m w.e.)	0.35	0.35	0.35
		RMSE (m w.e.)	0.45	0.45	0.45
		$R^2$	0.60	0.60	0.60
Scandinavia	355	MBE (m w.e.)	-0.06	-0.06	-0.06
		MAE (m w.e.)	0.61	0.61	0.62
		RMSE (m w.e.)	0.79	0.79	0.80
		$R^2$	0.43	0.44	0.42
Svalbard	112	MBE (m w.e.)	-0.16	-0.18	-0.18
		MAE (m w.e.)	0.39	0.32	0.33
		RMSE (m w.e.)	0.49	0.42	0.43
		$R^2$	0.13	0.35	0.33



220

**Figure 6: Histograms of the mass balance anomaly gradients  $\frac{db}{da}$  obtained from the leave-one-out cross-validation (LOOCV) experiment for the three study regions. Blue bars correspond to the European Alps, orange bars to Scandinavia, and green bars to Svalbard.**

#### 4.2 Improvement of geodetic mass balance estimates using MODIS albedo anomalies

225 To evaluate the added value of the albedo-anomaly method, we compared specific annual glacier mass balance estimates obtained by combining MODIS-derived glacier-wide albedo anomalies with geodetic specific mass balance data against estimates derived from geodetic data alone (Figure 7). The combined estimates were computed using the regionally derived gradients described in Sect. 4.1. Table 3 reports the associated error metrics for the three study regions.

Across all regions, incorporating MODIS albedo anomalies substantially improves the agreement with in-situ observations.

230 The RMSE decreases by 0.19 m w.e. in the European Alps, 0.23 m w.e. in Scandinavia, and 0.09 m w.e. in Svalbard. Similarly, the coefficient of determination  $R^2$  increases by 0.42, 0.38, and 0.30, respectively (Table 3).

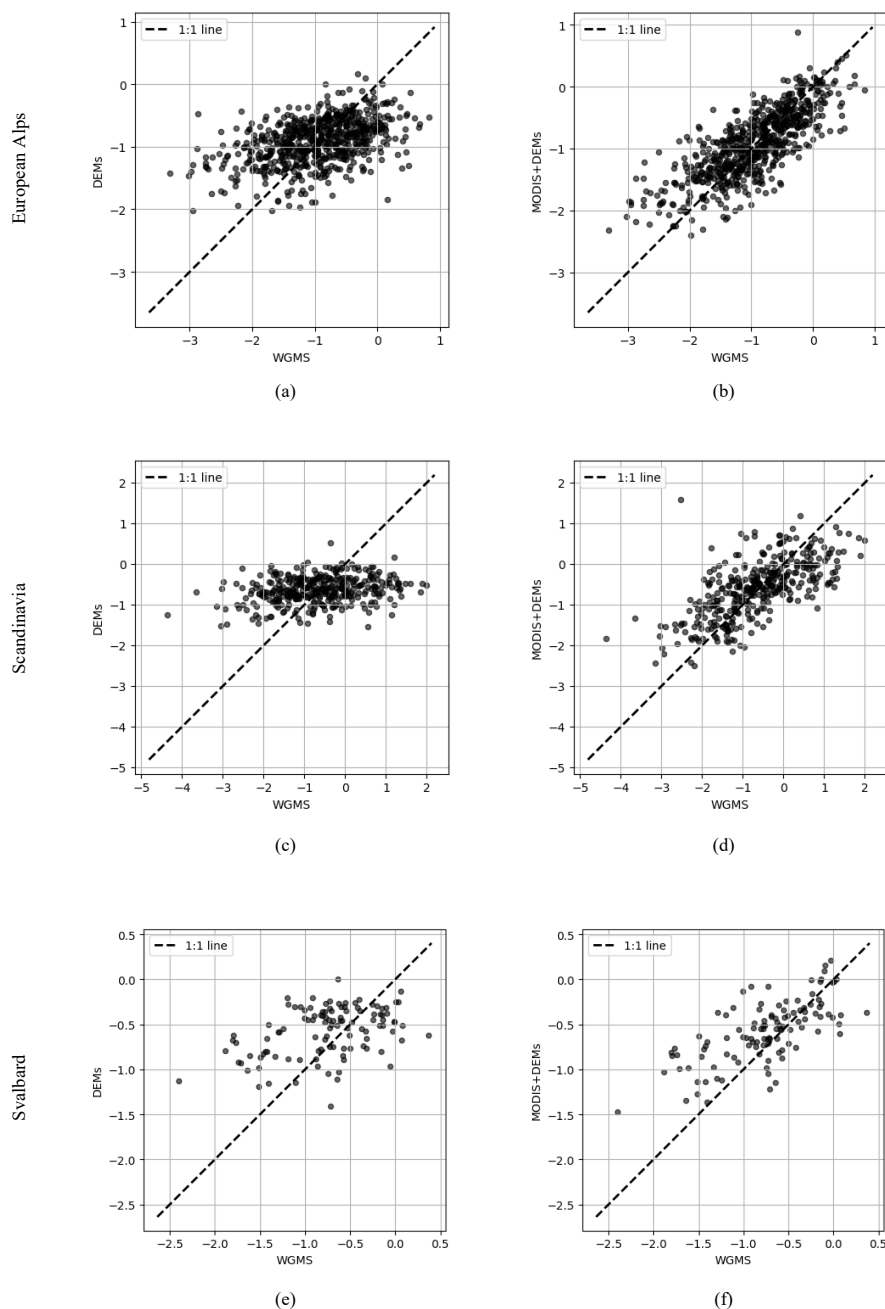


**Figure 7: Scatterplots comparing specific annual glacier mass balance derived from the reference glaciological method (WGMS dataset) with (a,c,e) geodetic estimates from DEMs (Hugonnet et al., 2021) and (b,d,f) estimates combining geodetic with MODIS albedo data (i.e. the proposed albedo-anomaly method) for the three test regions (a,b Alps; c,d Scandinavia; e,f Svalbard)**



**Table 3: Error metrics for the three regions, i.e. European Alps, Scandinavia and Svalbard between the reference glaciological method estimates (WGMS dataset) and those derived from DEMs (Hugonnet et al., 2021) and from the proposed albedo-anomaly method combining geodetic estimates with MODIS albedo data.**

Region	Number of validation samples	Error metric	DEMs	DEMs+MOD10
European Alps	641	MBE (m w.e.)	-0.06	-0.05
		MAE (m w.e.)	0.51	0.35
		RMSE (m w.e.)	0.64	0.45
		R <sup>2</sup>	0.18	0.60
Scandinavia	355	MBE (m w.e.)	-0.03	-0.06
		MAE (m w.e.)	0.83	0.61
		RMSE (m w.e.)	1.02	0.79
		R <sup>2</sup>	0.06	0.44
Svalbard	112	MBE (m w.e.)	-0.18	-0.18
		MAE (m w.e.)	0.42	0.32
		RMSE (m w.e.)	0.51	0.42
		R <sup>2</sup>	0.05	0.35

### 4.3 Regional annual mass balance time series

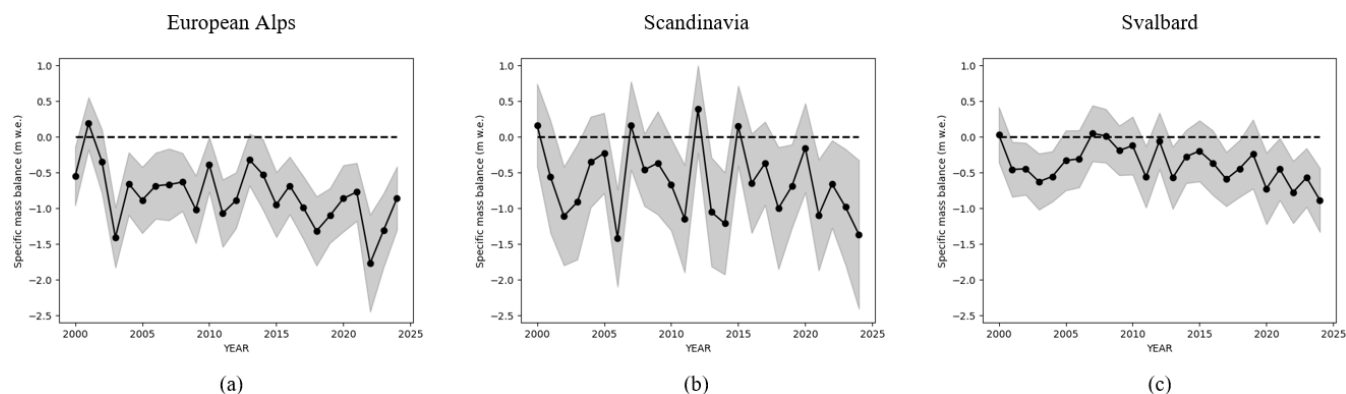
240 We computed annual specific glacier mass balance from 2000 to 2024 for all non-surging and land terminating glaciers larger than 0.5 km<sup>2</sup> using Eq. 1. Glaciers smaller than 0.5 km<sup>2</sup> were excluded to account for the spatial resolution limitations of the MOD10 albedo product (500 m). Surging and marine-terminating glaciers were also omitted, as their mass balance dynamics are influenced by processes, such as frontal ablation and surge-related mass redistribution, that weaken the relationship between surface albedo and mass balance. Table 4 summarizes the number of glaciers included in our analysis and compares this with the total number of glaciers reported in the RGI. Figure 8 shows the regional mean annual specific mass balance for the European Alps, Scandinavia, and Svalbard over the 2000–2024 period with shaded areas representing the inter-glacier variability within each region, expressed as one standard deviation.

250 **Table 4: Number of glaciers included in the regional annual specific mass balance time series analysis compared to the total number of glaciers reported in the Randolph Glacier Inventory (RGI v6.0). Only land-terminating, non-surging glaciers larger than 0.5 km<sup>2</sup> were retained, resulting in the percentages shown in parentheses for each study region.**

Region name	Total number of glaciers	Number of glaciers used in the time series (%)	Percentage of total glacier area analysed
European Alps	3892	689 (18%)	84 %
Scandinavia	3417	977 (28%)	86 %



Svalbard	1615	1082 (67%)	99%
----------	------	------------	-----



255 **Figure 8: Annual specific glacier mass balance time series estimated by using the proposed albedo-anomaly method for all non-surging and land terminating glaciers with extent larger than 0.5 km<sup>2</sup> in the Alps (a), Scandinavia (b), and Svalbard (c). Circular markers denote the average annual specific mass balance for each region, while the shaded areas represent the standard deviation, capturing the variability across all glaciers in each region. The horizontal dashed line represents the zero-mass balance.**

To assess the reliability of the estimated time series, we compared our results with the recently published dataset from Dussaillant et al. (2025). This dataset provides glacier-specific global annual mass balance estimates for the period 1976–2024, derived using geostatistical methods that integrate glaciological measurements with glacier-wide geodetic observations, including data from Hugonnet et al. (2021). The comparison was conducted using the same set of glaciers (see Table 4) to ensure consistency between the two methods. Overall, the two datasets show good agreement, with the general trends of mass balance variation captured consistently across regions (Figure 9). At the regional scale, the coefficient of determination ( $R^2$ ) between the two datasets is 0.69 for the European Alps, 0.74 for Scandinavia, and 0.61 for Svalbard, while the corresponding RMSE values are 0.39 m w.e., 0.42 m w.e., and 0.25 m w.e., respectively. These metrics indicate a generally strong correlation and reasonably small absolute differences, supporting the reliability of the albedo-anomaly estimates across diverse glacierized regions.

260

265

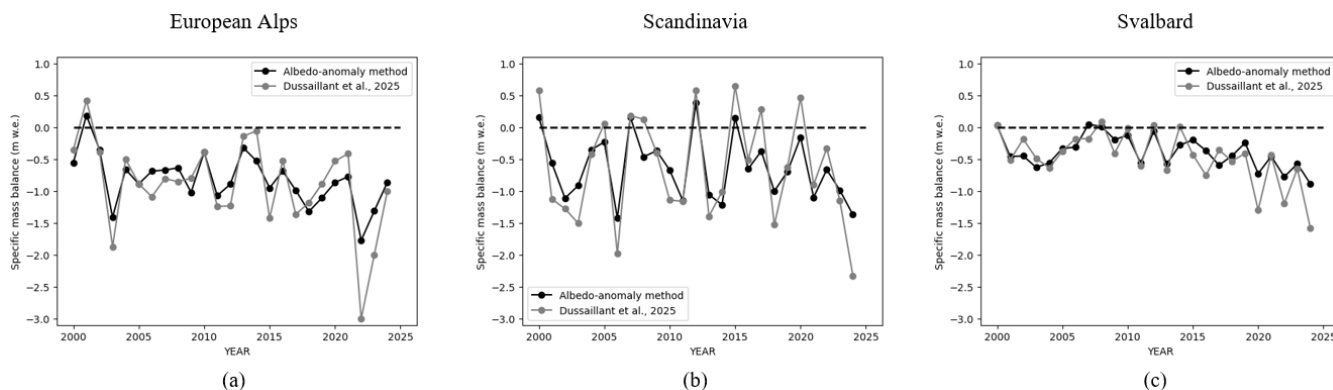


**Figure 9: Comparison of annual specific glacier mass balance time series derived from the albedo-anomaly method and the dataset from Dussaillant et al. (2025) for the European Alps, Scandinavia, and Svalbard. The same set of glaciers was used for both methods to ensure consistency.**

270

## 5. Discussion

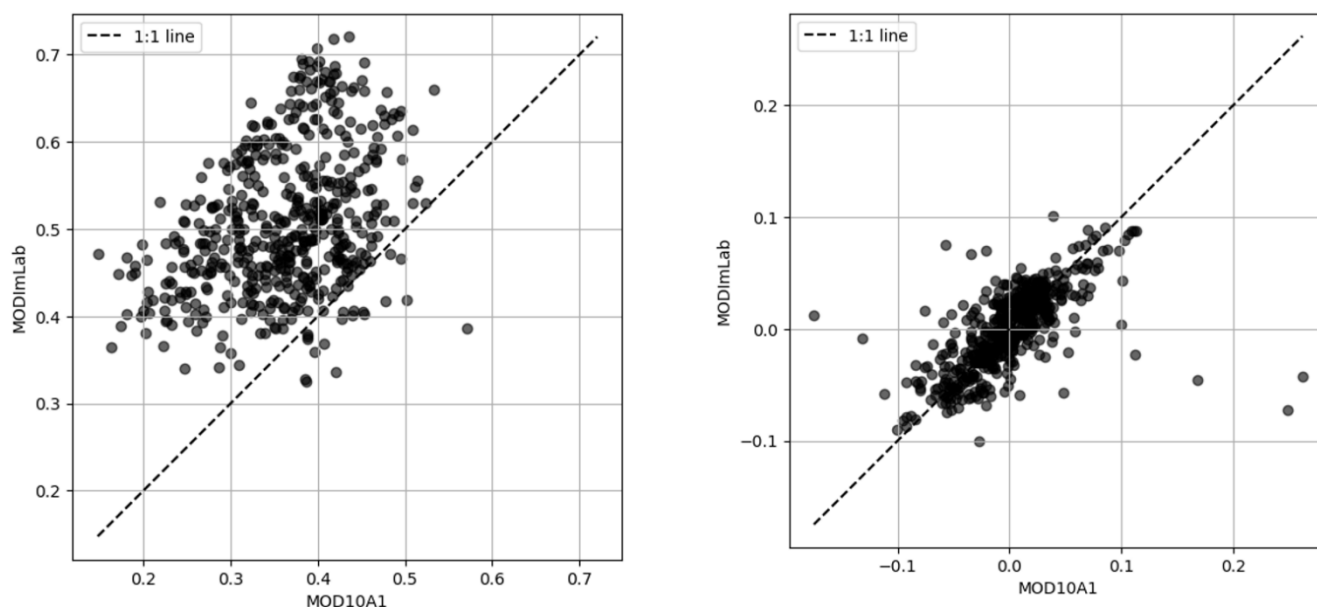
### 5.1 MODIS albedo product

Several studies have highlighted limitations in the use of the MOD10A1 albedo product for glacier surface analyses, primarily related to spatial resolution, cloud masking, topographic shading, and challenges in representing the complex anisotropic reflectance of bare ice compared to fresh snow (Dumont et al., 2012; Stroeve et al., 2006). To overcome some of these issues, Davaze et al. (2018) employed the MODImLab algorithm, specifically designed for glacier albedo monitoring, and produced snow and glacier albedo time series for the Mont Blanc region. In our study, we compared the mean summer albedo values derived from MOD10A1 with those obtained using the MODImLab product, following the same computational approach described in Section 3.1 to derive daily, glacier-wide albedo and aggregate these values into summer averages.

280

We performed this comparison for 30 glaciers in the Mont Blanc Massif over the period 2000–2016. As shown in Figure 10a, the absolute differences between the two datasets are considerable. These discrepancies can be attributed not only to the different retrieval algorithms employed, but also to differences in spatial resolution (250 m for MODImLab, versus 500 m for MOD10A1) and in the respective cloud-masking algorithm. However, when comparing albedo anomalies rather than absolute values, the discrepancies become much smaller, with RMSE equal to 0.03 and no systematic bias (Figure 10b). Since our analysis focuses on albedo anomalies and given that MOD10A1 is globally available and easily accessible through multiple platforms (e.g. GEE) we consider MOD10A1 to remain an appropriate and practical choice for the proposed albedo-anomaly method.

285



290 **Figure 10: Comparison between MOD10A1 and MODImLab (Davaze et al., 2018) glacier albedo estimates for 30 glaciers in the Mont Blanc Massif over the period 2000–2016. (a) Mean summer glacier-wide albedo derived from the two products. (b) Summer albedo anomalies from MOD10A1 and MODImLab, computed relative to the 2000–2016 reference period. The 1:1 line is shown for reference.**

## 5.2 Albedo-anomaly and glaciological methods

295 When comparing the albedo-anomaly estimates with glaciological measurements, the method performs well in both the European Alps and Svalbard, where RMSE on annual specific mass balance of 0.45 and 0.42 m w.e. are obtained (Table 3). These errors are of the same order as the typical uncertainties of glaciological surface mass balance measurements, generally ranging between 0.2 and 0.4 m w.e. (Rabatel et al., 2017). In Scandinavia, however, the method yields a higher RMSE of 0.79 m w.e., likely reflecting the reduced reliability of the 20-year geodetic estimates used for calibration in this region. This interpretation is consistent with the comparatively larger uncertainties associated with DEMs-only results in Scandinavia

300 (see Table 3), which propagate into the mass balance anomaly gradient (Eq. 1).

Dussaillant et al. (2025) recently proposed a complementary geostatistical approach that integrates glaciological measurements with geodetic data to spatialize annual mass balance. Although this method performs extremely well where in-situ observations are available, its accuracy decreases in regions far from monitored glaciers, due to the reduced influence

305 of field-based constraints. The albedo-anomaly method, by contrast, relies exclusively on satellite-derived inputs for the annual reconstruction of mass balance, enabling consistent estimates across entire regions once the anomaly–mass balance relationship has been calibrated. While this calibration still requires in-situ observations, the method can then propagate this information to remote, unmonitored glaciers. In this sense, the two approaches could be viewed as complementary: the geostatistical method provides highly accurate, observation-driven estimates where glaciological measurements are

310 available, whereas the albedo-anomaly method delivers spatially uniform performance across entire glacierized regions.



### 5.3 Albedo-anomaly and equilibrium line altitude methods

Our approach shares similarities with the Equilibrium Line Altitude (ELA) method, which combines annual snowline altitude (SLA) observations with decadal geodetic estimates to derive annual glacier mass balance. However, by utilizing a medium-resolution, daily dataset, specifically MODIS albedo, rather than the higher-resolution imagery (e.g., Landsat, Sentinel-2) typically used in the ELA method, our approach serves as a complementary alternative. The use of glacier-wide albedo integrated over the entire ablation season offers several advantages that address two key limitations of the ELA method. The first limitation is related to the SLA saturation effect, where the SLA reaches the maximum elevation of the glacier once the seasonal snow cover has fully melted. At this point, further changes in glacier mass balance are no longer reflected in SLA. In contrast, glacier-wide albedo integrated over the whole ablation season remains responsive to these conditions. Indeed, persistently low albedo values after the complete melt of snow cover serve as a clear indicator of low mass balance. The second limitation of the ELA method is related to cloud cover and data gaps. Estimating SLA requires high-resolution imagery from satellites such as Landsat or Sentinel-2. Especially prior to the launch of Sentinel-2, Landsat's 16-day revisit cycle, combined with frequent cloud cover, often resulted in sparse and incomplete SLA observations. MODIS albedo, with its daily temporal resolution, is significantly less affected by these limitations. On the other hand, the higher spatial resolution of snowline observations from Landsat or Sentinel-2 makes the ELA method more suitable for small glaciers, where MODIS's coarser resolution (500 m) is less effective.

Regarding the accuracy of glacier mass balance estimation, our proposed method performs similarly to the ELA method. For instance, Davaze et al. (2020) applied the ELA method using ASTER DEMs and Landsat-derived snowline observations, validating the results against glaciological measurements on 23 glaciers in the European Alps over the 2000–2016 period. They reported a RMSE of 0.6 m w.e. and a  $R^2$  of 0.33. In comparison, our method, validated over a longer period (2000–2019) and a broader sample of 42 glaciers in the same region, achieved a lower RMSE of 0.45 m w.e. and a higher  $R^2$  of 0.60. Although the datasets differ in terms of glacier selection and time span, we can fairly say that the two methods demonstrate comparable performances.

### 5.3 Satellite sensor limitations and potential future development

The spatial resolution of the geodetic dataset (100 m) and, more significantly, the MOD10A1 MODIS albedo product (500 m) limits the applicability of the method to large glaciers only. Consequently, in this study, we restricted the analysis to glaciers larger than 0.5 km<sup>2</sup>. The use of higher-resolution DEMs, such as those derived from airborne surveys or Pléiades imagery (Berthier et al., 2024), and high-resolution multispectral data, e.g., Landsat, Sentinel-2, for generating glacier-wide albedo time series (Naegli et al., 2017; Feng et al., 2024) could enable application to smaller glaciers. However, high resolution multi-spectral sensors typically lack daily temporal resolution (e.g., 16-day revisit for Landsat, 5-day for Sentinel-2). Therefore, strategies that integrate high-resolution imagery with daily, lower-resolution data should be considered for improved temporal coverage.



Another limitation related to satellite sensors is their longevity and future data availability. In late 2026/early 2027, the Terra satellite, which hosts both the ASTER and MODIS sensors, will begin shutting down operations. Future applications of the proposed method will require alternative sources for both geodetic measurements and multispectral observations. Potential options include stereoscopic imagery, e.g. Pléiades (Berthier et al., 2024), and InSAR-derived DEMs, e.g., TanDEM-X (Podgórski et al., 2019) for elevation change analysis. For multispectral observations, possible alternatives include OLCI and SLSTR sensors on board the Sentinel-3 satellite (Kokhanovsky et al., 2019) and VIIRS sensor on board the Suomi NPP (Zhou et al., 2016) satellites for daily coverage, as well as Landsat-8/9 and Sentinel-2 for higher spatial resolution (Naegli et al., 2017; Feng et al., 2024).

#### 5.4 Transferability to other regions

The albedo-anomaly method was applied to glaciers in the European Alps, Scandinavia, and Svalbard. Results demonstrate a clear benefit of incorporating glacier-wide albedo into decadal geodetic estimates, indicating a strong correlation between annual glacier-wide albedo anomalies and glacier mass balance anomalies in these regions. However, before extending the method to other parts of the world, it is essential to assess whether this relationship holds under different climatic and glaciological conditions. In-situ measurements are required to validate this assumption and to derive region-specific mass balance anomaly gradient, thereby improving the accuracy of the estimates.

At present, the albedo-anomaly method is not suitable for all glacier types. It cannot be reliably applied to small glaciers (<0.5 km<sup>2</sup>, see Section 5.3), surging glaciers, where dynamic changes can obscure the climatic signal captured by surface albedo, or marine-terminating glaciers, for which calibration with geodetic mass balance is biased due to unaccounted frontal ablation processes. These limitations should be considered when transferring the method beyond the regions investigated here.

## 6. Conclusion

We proposed a new method, i.e. the albedo-anomaly method, for estimating annual glacier mass balance by combining decadal geodetic mass balance estimates with MODIS-derived glacier-wide albedo time series. The method was applied to glaciers in the European Alps, Scandinavia, and Svalbard, resulting in annual mass balance time series from 2000 to 2024 for a total of 2748 glaciers. This dataset, which is publicly available, provides a valuable resource for studying glacier changes in these regions over the past 25 years.

To validate the method, we compared our estimates against 1108 in-situ measurements from 76 glaciers across the three regions. The resulting RMSE were 0.45, 0.79, and 0.42 m w.e. for the European Alps, Scandinavia, and Svalbard, respectively, with corresponding R<sup>2</sup> values of 0.60, 0.44, and 0.35.

As the albedo-anomaly method relies exclusively on satellite data, the method can be transferred to other glacierized regions worldwide, provided that sufficient in-situ data exist to calibrate region-specific mass-balance anomaly gradients. Its long-



term applicability will depend on future satellite missions, as the decommissioning of Terra will require replacing ASTER  
375 and MODIS with alternative geodetic and multispectral sources such as Pléiades, TanDEM-X, Sentinel-3 OLCI/SLSTR,  
VIIRS, and high-resolution missions like Sentinel-2 and Landsat-8/9.

The method contributes an important step toward expanding spatially complete, observation-driven glacier monitoring. By  
enabling regional-scale assessment of glacier response to climate variability, it strengthens our ability to quantify ongoing  
cryospheric change and its implications for water resources, sea-level rise, and climate feedbacks.

### 380 **Data and code availability**

The full implementation of the albedo-anomaly method is openly available at:

<https://github.com/mattiacallegari/albedo-anomaly-method>.

The annual glacier mass balance time series (2000–2024) for the 2,748 glaciers in the European Alps, Scandinavia, and  
Svalbard produced in this study can be accessed within the same repository at:

385 [https://github.com/mattiacallegari/albedo-anomaly-method/tree/main/data/albedo-anomaly\\_method\\_annual\\_gmb](https://github.com/mattiacallegari/albedo-anomaly-method/tree/main/data/albedo-anomaly_method_annual_gmb).

### **Acknowledgments**

This research was financed by the Research Council of Norway under the “Researcher Project for Scientific Renewal”  
(project MASSIVE, no. 315971). The authors thank Marie Dumont and Antoine Rabatel for kindly sharing the MODImLab  
albedo dataset used for comparison with the MOD10A1 product.

### 390 **Author contributions**

MC and TS designed the research. MC implemented the code for data preparation and processing. All authors contributed to  
the design of the experiments and to the analysis and interpretation of the results. MC wrote the manuscript with input and  
feedback from all co-authors.

### **Competing interests**

395 The authors declare that they have no competing interest.



## References

- Andreassen, L. M., Elvehøy, H., Kjøllmoen, B., Belart, J. M. C.: Glacier change in Norway since the 1960s – an overview of mass balance, area, length and surface elevation changes, *J. Glaciol.*, 66 (256), 313–328., <https://doi.org/10.1017/jog.2020.10>, 2020.
- 400 Berthier, E., Lebreton, J., Fontannaz, D., Hosford, S., Belart, J. M.-C., Brun, F., Andreassen, L. M., Menounos, B., and Blondel, C.: The Pléiades Glacier Observatory: high-resolution digital elevation models and ortho-imagery to monitor glacier change, *Cryosph.*, 18, 5551–5571, <https://doi.org/10.5194/tc-18-5551-2024>, 2024.
- Brun, F., Dumont, M., Wagnon, P., Berthier, E., Azam, M. F., Shea, J. M., Sirguey, P., Rabatel, A., and Ramanathan, A.: Seasonal changes in surface albedo of Himalayan glaciers from MODIS data and links with the annual mass balance, *Cryosph.*, 9, 341–355, <https://doi.org/10.5194/tc-9-341-2015>, 2015.
- 405 Cogley, J. G., Hock, R., Rasmussen, L. A., Arendt, A. A., Bauder, A., Braithwaite, R. J., Jansson, P., Kaser, G., Möller, M., and Nicholson, L.: Glossary of glacier mass balance and related terms, IHP-VII Tech. Doc. Hydrol., 86, 2011.
- Davaze, L., Rabatel, A., Arnaud, Y., Sirguey, P., Six, D., Letreguilly, A., and Dumont, M.: Monitoring glacier albedo as a proxy to derive summer and annual surface mass balances from optical remote-sensing data, *Cryosph.*, 12, 271–286, <https://doi.org/10.5194/tc-12-271-2018>, 2018.
- 410 Davaze, L., Rabatel, A., Dufour, A., Hugonnet, R., and Arnaud, Y.: Region-Wide Annual Glacier Surface Mass Balance for the European Alps From 2000 to 2016, *Front. Earth Sci.*, 8, <https://doi.org/10.3389/feart.2020.00149>, 2020.
- Dumont, M., Gardelle, J., Sirguey, P., Guillot, A., Six, D., Rabatel, A., and Arnaud, Y.: Linking glacier annual mass balance and glacier albedo retrieved from MODIS data, *Cryosph.*, 6, 1527–1539, <https://doi.org/10.5194/tc-6-1527-2012>, 2012.
- 415 Dussaillant, I., Hugonnet, R., Huss, M., Berthier, E., Bannwart, J., Paul, F., and Zemp, M.: Annual mass change of the world’s glaciers from 1976 to 2024 by temporal downscaling of satellite data with in situ observations, *Earth Syst. Sci. Data*, 17, 1977–2006, <https://doi.org/10.5194/essd-17-1977-2025>, 2025.
- Feng, S., Cook, J. M., Onuma, Y., Naegeli, K., Tan, W., Anesio, A. M., Benning, L. G. and Tranter, M.: Remote sensing of ice albedo using harmonized Landsat and Sentinel-2 datasets: validation, *Int. J. Remote Sens.*, 45, 7724–7752, <https://doi.org/10.1080/01431161.2023.2291000>, 2024
- 420 Greuell, W. and Oerlemans, J.: Assessment of the surface mass balance along the K-transect (Greenland ice sheet) from satellite-derived albedos, *Ann. Glaciol.*, 42, 107–117, <https://doi.org/10.3189/172756405781812682>, 2005.
- Greuell, W., Kohler, J., Obleitner, F., Glowacki, P., Melvold, K., Bernsen, E., and Oerlemans, J.: Assessment of interannual variations in the surface mass balance of 18 Svalbard glaciers from the Moderate Resolution Imaging Spectroradiometer/Terra albedo product, *J. Geophys. Res. Atmos.*, 112, <https://doi.org/10.1029/2006JD007245>, 2007.
- 425 Hall, D. K. and Riggs, G. A.: MODIS/Terra CGF Snow Cover Daily L3 Global 500m SIN Grid, Version 61 [Data Set]. Boulder, Colorado USA., <https://doi.org/10.5067/MODIS/MOD10A1.061>, 2021.



- Hugonnet, R., McNabb, R., Berthier, E., Menounos, B., Nuth, C., Girod, L., Farinotti, D., Huss, M., Dussailant, I., Brun, F., and Kääb, A.: Accelerated global glacier mass loss in the early twenty-first century, *Nature*, 592, 726–731, 430 <https://doi.org/10.1038/s41586-021-03436-z>, 2021.
- Huss, M. and Hock, R.: Global-scale hydrological response to future glacier mass loss, *Nat. Clim. Chang.*, 8, 135–140, <https://doi.org/10.1038/s41558-017-0049-x>, 2018.
- Kokhanovsky, A. A., Lamare, M., Danne, O., Brockmann, C., Dumont, M., Picard, G., Arnaud, L., Favier, V., Jourdain, B., Le Meur, E., Di Mauro, B., Aoki, T., Niwano, M., Rozanov, V., Korkin, S., Kipfstuhl, S., Freitag, J., Hoerhold, M., Zuhr, A., 435 Vladimirova, D. O., Faber, A.-K., Steen-Larsen, H. C., Wahl, S., Andersen, J. K., Vandecrux, B., van As, D., Mankoff, K. D., Kern, M., Zege, E., and Box, J. E.: Retrieval of snow properties from the Sentinel-3 Ocean and Land Colour Instrument, *Remote Sens.*, 11, 2280, <https://doi.org/10.3390/rs11192280>, 2019.
- Naegeli, K., Damm, A., Huss, M., Wulf, H., Schaepman, M. E., and Hoelzle, M.: Cross-comparison of albedo products for glacier surfaces derived from airborne and satellite (Sentinel-2 and Landsat 8) optical data, *Remote Sens.*, 9, 110, 440 <https://doi.org/10.3390/rs9020110>, 2017
- Marzeion, B., Jarosch, A. H., and Hofer, M.: Past and future sea-level change from the surface mass balance of glaciers, *Cryosph.*, 6, 1295–1322, <https://doi.org/10.5194/tc-6-1295-2012>, 2012.
- Di Mauro, B. and Fugazza, D.: Pan-Alpine glacier phenology reveals lowering albedo and increase in ablation season length, *Remote Sens. Environ.*, 279, 113119, <https://doi.org/10.1016/j.rse.2022.113119>, 2022.
- 445 Maussion, F., Butenko, A., Champollion, N., Dusch, M., Eis, J., Fourteau, K., Gregor, P., Jarosch, A. H., Landmann, J., Oesterle, F., Recinos, B., Rothenpieler, T., Vlug, A., Wild, C. T., and Marzeion, B.: The Open Global Glacier Model (OGGM) v1.1, *Geosci. Model Dev.*, 12, 909–931, <https://doi.org/10.5194/gmd-12-909-2019>, 2019.
- Podgórski, J., Kinnard, C., Pętllicki, M., and Urrutia, R.: Performance assessment of TanDEM-X DEM for mountain glacier elevation change detection, *Remote Sens.*, 11, 187, <https://doi.org/10.3390/rs11020187>, 2019.
- 450 Rabatel, A., Dedieu, J. P., and Vincent, C.: Using remote-sensing data to determine equilibrium-line altitude and mass-balance time series: Validation on three French glaciers, 1994-2002, *J. Glaciol.*, 51, 539–546, <https://doi.org/10.3189/172756505781829106>, 2005.
- Rabatel, A., Bermejo, A., Loarte, E., Soruco, A., Gomez, J., Leonardini, G., Vincent, C., and Sicart, J. E.: Can the snowline be used as an indicator of the equilibrium line and mass balance for glaciers in the outer tropics?, *J. Glaciol.*, 58, 1027–1036, 455 <https://doi.org/10.3189/2012JoG12J027>, 2012.
- Rabatel, A., Dedieu, J. P., and Vincent, C.: Spatio-temporal changes in glacier-wide mass balance quantified by optical remote sensing on 30 glaciers in the French Alps for the period 1983-2014, *J. Glaciol.*, 62, 1153–1166, <https://doi.org/10.1017/jog.2016.113>, 2016.
- Rabatel, A., Sirguey, P., Drolon, V., Maisongrande, P., Arnaud, Y., Berthier, E., Davaze, L., Dedieu, J.-P., and Dumont, M.: 460 Annual and Seasonal Glacier-Wide Surface Mass Balance Quantified from Changes in Glacier Surface State: A Review on Existing Methods Using Optical Satellite Imagery, *Remote Sens.*, 9, 507, <https://doi.org/10.3390/rs9050507>, 2017.



- RGI Consortium: Randolph Glacier Inventory 6.0, <https://doi.org/10.7265/n5-rgi-60>, 2017.
- De Ruyter De Wildt, M. S., Oerlemans, J., and Björnsson, H.: A method for monitoring glacier mass balance using satellite albedo measurements: application to Vatnajökull, Iceland, *J. Glaciol.*, 48, 267–278, <https://doi.org/10.3189/172756502781831458>, 2002.
- Schmidt, L. S., Schuler, T. V., Thomas, E. E., and Westermann, S.: Meltwater runoff and glacier mass balance in the high Arctic: 1991–2022 simulations for Svalbard, *Cryosph.*, 17, 2941–2963, <https://doi.org/10.5194/tc-17-2941-2023>, 2023.
- Sirguey, P., Still, H., Cullen, N. J., Dumont, M., Arnaud, Y., and Conway, J. P.: Reconstructing the mass balance of Brewster Glacier, New Zealand, using MODIS-derived glacier-wide albedo, *Cryosph.*, 10, 2465–2484, <https://doi.org/10.5194/tc-10-2465-2016>, 2016.
- Stroeve, J. C., Box, J. E., and Haran, T.: Evaluation of the MODIS (MOD10A1) daily snow albedo product over the Greenland ice sheet, *Remote Sens. Environ.*, 105, 155–171, <https://doi.org/10.1016/j.rse.2006.06.009>, 2006.
- Williamson, S. N., Marshall, S. J., and Menounos, B.: Temperature mediated albedo decline portends acceleration of North American glacier mass loss, *Commun. Earth Environ.*, 6, 555, <https://doi.org/10.1038/s43247-025-02503-x>, 2025.
- 465 Zemp, M., Huss, M., Thibert, E., Eckert, N., McNabb, R., Huber, J., Barandun, M., Machguth, H., Nussbaumer, S. U., Gärtner-Roer, I., Thomson, L., Paul, F., Maussion, F., Kutuzov, S., and Cogley, J. G.: Global glacier mass changes and their contributions to sea-level rise from 1961 to 2016, *Nature*, 568, 382–386, <https://doi.org/10.1038/s41586-019-1071-0>, 2019.
- 470 Zhou, Y., Wang, D., Liang, S., and He, T.: Assessment of the Suomi NPP VIIRS land surface albedo data using station measurements and high-resolution albedo maps, *Remote Sens.*, 8, 137, <https://doi.org/10.3390/rs8020137>, 2016.
- 480 The GlaMBIE Team: Community estimate of global glacier mass changes from 2000 to 2023, *Nature*, 639, 382–388, <https://doi.org/10.1038/s41586-024-08545-z>, 2025.